
Article:
Cunningham, V.J., Ning, Y., Armes, S.P. orcid.org/0000-0002-8289-6351 et al. (1 more author) (2016) Poly(N-2-(methacryloyloxy)ethyl pyrrolidone)-poly(benzyl methacrylate) diblock copolymer nano-objects via RAFT alcoholic dispersion polymerisation in ethanol. Polymer, 106. pp. 189-199. ISSN 0032-3861

https://doi.org/10.1016/j.polymer.2016.07.072

Poly(*N*-2-(methacryloyloxy)ethyl pyrrolidone)-poly(benzyl methacrylate) diblock copolymer nano-objects via RAFT alcoholic dispersion polymerisation in ethanol

Victoria J. Cunningham,[a] Yin Ning,[a] Steven P. Armes[a*] and Osama M. Musa[b]

a. Department of Chemistry, University of Sheffield, Brook Hill, Sheffield, South Yorkshire, S3 7HF, UK.

b. Ashland Specialty Ingredients, 1005 US 202/206, Bridgewater, NJ 08807, USA.

Key words: block copolymer nanoparticles, dispersion polymerisation, polymerisation-induced self-assembly

Abstract. *N*-2-(Methacryloyloxy)ethyl pyrrolidone (NMEP) is a highly polar monomer that is much more readily copolymerised with methacrylic monomers than its structural analogue, *N*-vinyl pyrrolidone. The RAFT solution polymerisation of NMEP has been conducted in ethanol at 70 °C while varying the degree of polymerisation (DP) from 70 to 400. Reducing the CTA/initiator molar ratio from 10.0 to 3.0 when targeting $PNMEP_{100}$ led to a three-fold rate enhancement and increased the final monomer conversion from 72 % to 98 %. Targeting DPs of 200 or greater led to lower monomer conversions. DMF GPC analysis of a series of $PNMEP_x$ homopolymers confirmed a linear increase in molecular weight with conversion and relatively low dispersities (M_w/M_n < 1.26). A $PNMEP_{50}$ macro-CTA was chain-extended with benzyl methacrylate (BzMA) via RAFT alcoholic dispersion polymerisation. High BzMA conversions (> 90 %) were obtained and electron microscopy studies indicated that a range of diblock copolymer morphologies, e.g. spheres, worms and vesicles, were produced by polymerisation-induced self-assembly (PISA). Finally, a $PNMEP_{47}$-$PBzMA_{243}$ diblock copolymer was synthesised via a convenient 'one-pot' protocol whereby a $PNMEP_{47}$ macro-CTA was first prepared at 97% conversion, followed by *in situ* RAFT dispersion polymerisation of BzMA to produce diblock copolymer nano-objects. TEM analysis of aliquots taken during the diblock copolymer synthesis indicated a gradual evolution in copolymer morphology from spherical micelles after 1 h to a pure vesicle phase after 8 h via intermediate mixed phases (including worms).

* Author to whom correspondence should be addressed (s.p.armes@sheffield.ac.uk)

Introduction

In recent years, controlled radical polymerisation techniques such as atom transfer radical polymerisation (ATRP)[1-3], nitroxide-mediated polymerisation (NMP)[4] and reversible addition-fragmentation chain transfer (RAFT) polymerisation [5-11] have dominated the synthetic polymer chemistry literature. In particular, RAFT polymerisation is extremely versatile and offers a convenient route to well-controlled homopolymers and diblock copolymers for a wide range of vinyl monomers. When combined with the well-established principle of polymerisation-induced self-assembly (PISA),[12-15] RAFT polymerisation has enabled the rational synthesis of diblock copolymer nano-objects in various media, including water,[13, 16-20] *n*-alkanes,[21-27] ionic liquids [28] and lower alcohols.[29-36]

Pan and co-workers have made a number of notable contributions to the field of RAFT alcoholic dispersion polymerisation [37-40]. Their approach typically involves chain extension of a soluble macro-CTA such as poly(2-dimethylaminoethyl methacrylate) with styrene in methanol [37]. Good control over the molecular weight distribution can be achieved, but relatively low styrene conversions are usually obtained (e.g. < 70% after 36 h at 80 ^{o}C). A range of diblock copolymer nano-objects are generated via PISA as the growing polystyrene block becomes insoluble [12, 15]. Pure phases of spherical micelles, worm-like micelles or vesicles can be obtained simply by varying the feed ratios and reaction conditions [37]. To address the problem of incomplete monomer conversion for the core-forming block, both Charleux's group[41] and Armes and co-workers[30, 33, 42] have explored replacing styrene with benzyl methacrylate (BzMA). This approach leads to substantially higher conversions (84-100%)[29, 30, 33, 36]. For example, Semsarilar et al. examined the following four alcohol-soluble macromolecular chain transfer agents (macro-CTAs) as stabiliser blocks: poly(2-dimethylaminoethyl methacrylate), poly(methacrylic acid), poly(glycerol monomethacrylate) and poly(2-(methacryloyloxy)ethyl phosphorylcholine). Chain extension of each precursor with benzyl methacrylate in either ethanol or methanol led to high conversions (> 92 %) in each case while systematic variation of the target degree of polymerisation (DP) for the PBzMA block produced a range of copolymer morphologies as judged by transmission electron microscopy (TEM).[29] Various research groups have studied the effect of addition of water to such RAFT alcoholic dispersion polymerisation formulations [36, 41, 43, 44]. This co-solvent invariably causes a dramatic rate acceleration but tends to limit the final block copolymer morphology to kinetically-trapped spheres [36, 41].

N-2-(methacryloyloxy)ethyl pyrrolidone (NMEP) has been recently studied in the context of RAFT solution polymerisation [45-48]. For example, Deng et al. prepared three PNMEP-based diblock

copolymers by chain-extending a PNMEP macro-CTA with either glycidyl methacrylate, oligo(ethylene glycol) monomethacrylate or 2-(dimethylamino)ethyl methacrylate in methanol at 30 °C using visible light-mediated RAFT polymerisation. The resulting diblock copolymers exhibited high blocking efficiencies but relatively poor conversions for the second block (typically less than 50%)[45]. In related work, Zhang et al. synthesised a poly(lauryl methacrylate) macro-CTA and chain-extended it in chloroform to produce a series of poly(lauryl methacrylate)-poly(*N*-2-(methacryloyloxy)ethyl pyrrolidone) (PLMA-PNMEP) diblock copolymers via RAFT solution polymerisation [47]. NMEP conversions of 56 to 63 % were reported and post-polymerisation processing via a solvent switch led to the formation of PLMA-PNMEP diblock copolymer spheres in THF. We recently reported the first example of utilising NMEP in a PISA formulation [48]. A range of poly(stearyl methacrylate)-poly(*N*-(2-(methacryloyloxy)ethyl pyrrolidone) (PSMA-PNMEP) diblock copolymer nano-objects were prepared via RAFT dispersion polymerisation of NMEP using a PSMA macro-CTA in *n*-dodecane at 90 °C [48]. Relatively high conversions (> 95 %) were achieved and the construction of a suitable phase diagram enabled the reproducible targeting of either spheres, worms or vesicles. In this case, the PNMEP formed the structure-directing insoluble block; as far as we are aware, there have been no literature examples of using PNMEP as a stabiliser block for PISA syntheses.

In the present study, the effect of varying the target DP and the RAFT CTA/initiator molar ratio on the kinetics of the RAFT solution homopolymerisation of NMEP in ethanol is examined. The RAFT alcoholic dispersion polymerisation of BzMA using a PNMEP macro-CTA is assessed as a potential route to a series of sterically-stabilised PNMEP-PBzMA diblock copolymer nano-objects. The resulting diblock copolymer chains are characterised by ^{1}H NMR spectroscopy and DMF GPC and the copolymer morphology is analysed by electron microscopy. Finally, a one-pot PISA formulation for the production of such diblock copolymer nano-objects is explored.

Experimental

Materials

N-(2-(methacryloyloxy)ethyl pyrrolidone) (NMEP) was kindly donated by Ashland Specialty Ingredients (New Jersey, USA) and was used as received. Benzyl methacrylate (BzMA) and 4,4'-azobis(4-cyanopentanoic acid) (ACVA) were purchased from Sigma-Aldrich (Dorset, UK) and were used as received. 2-Cyano-2-propyl dithiobenzoate (CPDB) was purchased from Strem Chemicals Ltd. (Cambridge, UK) and was used as received. d_4-Methanol was purchased from Goss Scientific

Instruments Ltd (Cheshire, UK) and *d*-chloroform was purchased from VWR chemicals (UK) and were used as received. All other solvents were purchased from Fisher Scientific (Loughborough, UK).

Kinetics of the RAFT solution homopolymerisation of NMEP in ethanol

A typical protocol for the RAFT solution homopolymerisation of NMEP when targeting $PNMEP_{100}$ was conducted as follows. NMEP (4.6473 g, 23.563 mmol), CPDB RAFT agent (0.0499 g, 0.225 mmol; target DP = 100), ACVA (12.5 mg, 44.598 µmol; CPDB/ACVA molar ratio = 5.0) and ethanol (6.9540 g, 40% w/w) were weighed into a 28 ml vial. The reaction solution was stirred and degassed in an ice bath for 30 min before being placed in an oil bath at 70 °C. The polymerisation was sampled every 30 min for the first 4 h and then every 60 min for a total of 10 h. Each aliquot was analysed by ^{1}H NMR spectroscopy and DMF GPC. A range of other $PNMEP_x$ homopolymers were prepared by either varying the CPDB/ACVA molar ratio or the CPDB/NMEP molar ratio.

Synthesis of a $PNMEP_{50}$ macro-CTA

NMEP (33.4012 g, 0.17 mol), CPDB RAFT agent (1.0006 g, 4.52 mmol; target DP = 45), ACVA (337.8 mg, 1.21 mmol; CPDB/ACVA molar ratio = 3.0) and ethanol (22.2815 g, 60% w/w solids) were weighed into a 250 ml round-bottom flask. The reaction solution was stirred and degassed in an ice bath for 45 min before being placed in an oil bath at 70 °C. The polymerisation was allowed to proceed for 5.75 h, resulting in a monomer conversion of 91 % as judged by ^{1}H NMR. The crude homopolymer was purified by precipitating into a ten-fold excess of diethyl ether. This purification protocol was repeated twice. The purified PNMEP macro-CTA was dissolved in the minimum volume of water and this concentrated aqueous solution was freeze-dried overnight to afford a pure PNMEP macro-CTA (< 1 % residual monomer). The mean DP was calculated using ^{1}H NMR to be 50 by comparing the integrated aromatic proton signals at 7-8 ppm to that of the methylene carbonyl proton signal at 2.5 ppm. DMF GPC analysis indicated a M_n of 8,000 g mol^{-1} and a M_w/M_n of 1.15 (compared to a series of near-monodisperse poly(methyl methacrylate) calibration standards).

RAFT alcoholic dispersion polymerisation of BzMA using a $PNMEP_{50}$ macro-CTA

A typical protocol for the synthesis of $PNMEP_{50}$-$PBzMA_{47}$ diblock copolymer nanoparticles was conducted as follows: $PNMEP_{50}$ macro-CTA (0.3607 g), BzMA (0.3124 g, 1.77 mmol; target DP = 50) and ACVA (2.0 mg, 7.13 µmol; macro-CTA/ACVA molar ratio = 5.0) were dissolved in ethanol (2.6948 g, 20% w/w) in a 14 ml vial. The reaction mixture was sealed and purged in an ice bath with nitrogen for 30 min, prior to immersion in an oil bath set at 70 °C for 24 h. The resulting crude copolymer was analysed by DMF GPC (M_n = 12 000 g mol^{-1}, M_w/M_n = 1.20). ^{1}H NMR spectroscopy analysis of the final

reaction solution (diluted in $CDCl_3$) indicated 94 % BzMA conversion. Other diblock copolymer compositions were obtained by systematically adjusting the BzMA/$PNMEP_{50}$ macro-CTA molar ratio to give target PBzMA DPs ranging from 50 to 250.

PISA synthesis of $PNMEP_{47}$-$PBzMA_{243}$ diblock copolymer nano-objects via a one-pot protocol

NMEP (4.6480 g, 0.024 mol), CPDB RAFT agent (0.1250 g, 0.565 mmol; target DP = 250), ACVA (42.1 mg, 0.150 mmol; CPDB/ACVA molar ratio = 3.0) and ethanol (3.0844 g, 60% w/w solids) were weighed into a 28 ml vial. The reaction solution was stirred and degassed in an ice bath for 30 min before being placed in an oil bath at 70 °C. The polymerisation was sampled every 30 min for 4 h and sampled thereafter every 60 min up to 6 h, resulting in 97 % BzMA conversion and an PNMEP DP of 47 as determined by ^{1}H NMR. A portion of the crude $PNMEP_{47}$ macro-CTA solution (1.0002 g at 60% w/w solids) was diluted with a degassed mixture of BzMA (2.7832, 15.795 mmol), ACVA (0.0034 g, 0.121 mmol) and ethanol (7.5363 g, 30% w/w solids). The reaction mixture was sampled every 60 min for 10 h. Each aliquot was analysed by DMF GPC and ^{1}H NMR. A final BzMA conversion of 97% was obtained after 24 h at 70 °C.

Copolymer characterisation

^{1}H NMR Spectroscopy. All ^{1}H NMR spectra were recorded using a 400 MHz Bruker Avance-400 spectrometer using either CD_3OD or $CDCl_3$.

Gel Permeation Chromatography (GPC). The molecular weights and dispersities of the various PNMEP homopolymers and $PNMEP_{50}$-$PBzMA_x$ diblock copolymers were determined by DMF GPC at 60 °C. The GPC set-up consisted of two Polymer Laboratories PL gel 5 μm Mixed C columns connected in series to a Varian 390 LC multidetector suite (refractive index detector) and a Varian 290 LC pump injection module. The mobile phase was HPLC-grade DMF containing 10 mmol LiBr and the flow rate was 1.0 ml min^{-1}. A series of ten near-monodisperse poly(methyl methacrylate) (PMMA) samples were used as calibration standards and DMSO was used as a flow rate marker. Data were analysed using Varian Cirrus GPC software (version 3.3).

Transmission Electron Microscopy (TEM). Copper/palladium TEM grids (Agar Scientific, UK) were coated in-house to yield a thin film of amorphous carbon. The grids were subjected to a glow discharge for 30 seconds to create a hydrophilic surface. Dilute solutions (0.20% w/w in ethanol, 10.0 μL) were adsorbed onto the carbon-coated grids for 1 min and then blotted with filter paper to remove excess solution. Uranyl formate (9.0 μL of a 0.75% w/w solution) was absorbed onto the sample-loaded grid for 20 seconds and then blotted to remove excess stain. The grids were then

dried with a vacuum hose. Imaging was performed using a Philips CM100 instrument operating at 100 kV and equipped with a Gatan 1 k CCD camera.

Scanning Electron Microscopy (SEM). Samples were analysed using a FEI Inspect F scanning electron microscope at 10 kV. All samples were gold-coated for ~ 60 seconds using a current of 15 mA prior to imaging to prevent sample charging.

Results and discussion

Kinetics of the RAFT solution homopolymerisation of NMEP in ethanol at 70^{o}C

Compared to related pyrrolidone-functional monomers such as *N*-vinyl pyrrolidone,[49-54] there are rather few literature reports describing the RAFT polymerisation of NMEP [45-48]. Thus, a detailed study of the kinetics of the RAFT solution homopolymerisation of PNMEP in ethanol at 70 °C was conducted. The NMEP concentration was fixed at 40% w/w solids in these experiments, while the RAFT CTA/initiator molar ratio and the target DP were systematically varied.

Initially, a PNMEP DP of 100 was targeted to study the effect of systematically increasing the CPDB/ACVA molar ratio from 3.0 to 10.0. Each reaction was sampled every 30 min for the first 4 h and then every 60 min for 10 h. Each polymerisation was terminated after 24 h. Aliquots were analysed by ^{1}H NMR and DMF GPC analysis. Figure 1a shows the monomer conversion vs. time curves obtained when using four different CPDB/ACVA molar ratios. As expected, a CPDB/ACVA molar ratio of 3.0 led to very fast kinetics, with more than 90 % NMEP conversion observed within 8 h at 70 °C and 98% conversion being achieved after 24 h. In contrast, a CPDB/ACVA molar ratio of 10.0 led to a much slower polymerisation: only 58% conversion was achieved after 10 h (and a final conversion of 72% after 24 h). CPDB/ACVA molar ratios of 5.0 or 7.0 gave intermediate behaviour. Figure 1a clearly also indicates longer induction times are obtained when employing higher CPDB/ACVA molar ratios. Figure 1b, shows the corresponding semi-logarithmic plots obtained for the four kinetic data sets when targeting PNMEP$_{100}$. After the initial induction period, first order kinetics with respect to monomer are observed, with higher pseudo-first order rate constants being obtained for lower CPDB/ACVA molar ratios. In each case, deviations from linearity occur prior to full conversion. For a CPDB/ACVA molar ratio of 3.0, a linear relationship is maintained up to 86% conversion, whereas non-linear behaviour is observed above approximately 60% conversion for the other three data sets.

Figure S1 shows the DMF GPC data for the same four sets of PNMEP$_{100}$ kinetic data. A linear increase in number-average molecular weight (M_n) with NMEP conversion is observed, as expected for a well-controlled RAFT polymerisation [8]. Relatively low dispersities are obtained throughout each

polymerisation, with final M_w/M_n values of less than 1.26 (data not shown). This is perhaps surprising for the relatively low CPDB/ACVA molar ratio of 3.0 since it is well-known that higher initiator concentrations can often lead to a lack of control [40, 55].

Next, the effect of varying the target PNMEP DP on the homopolymer kinetics in ethanol at 40% w/w solids and 70 °C was studied. Four PNMEP DPs were targeted, ranging from 70 to 400. A constant CPDB/ACVA molar ratio of 5.0 was used for these syntheses. Again, aliquots were taken from the polymerising solution every 30 min for the first 4 h and then every 60 min for 10 h. Figure 2a shows the four monomer conversion vs. time curves. In each case, an induction period of approximately 1 h is observed. Targeting a PNMEP DP of either 70 or 100 led to conversions of more than 90% being achieved after 24 h, whereas higher target PNMEP DPs led to somewhat lower conversions. DMF GPC was used to assess the evolution in molecular weight during these polymerisations, see Figure 2b. A linear increase in molecular weight with conversion was observed in each case. As expected, the target PNMEP DP of 400 exhibits the highest final M_n, with an appropriate reduction in M_n being observed when targeting the lower PNMEP DPs.

RAFT alcoholic dispersion polymerisation of BzMA using a $PNMEP_{50}$ macro-CTA

A $PNMEP_{50}$ macro-CTA was first prepared via RAFT solution polymerisation of NMEP in ethanol at 70 °C using a CPDB/ACVA molar ratio of 3.0 and targeting a DP of 45. This macro-CTA was purified by repeated precipitation into diethyl ether: ^{1}H NMR spectroscopy studies confirmed that there was negligible residual monomer and end-group analysis of the aromatic proton signals assigned to the RAFT chain-ends indicated a mean DP of 50 (91% conversion). DMF GPC analysis of the $PNMEP_{50}$ macro-CTA indicated an M_n of 8,000 g mol^{-1} and a relatively low dispersity of 1.15.

This $PNMEP_{50}$ macro-CTA was subsequently utilised for the synthesis of $PNMEP_{50}$-$PBzMA_{200}$ diblock copolymer nanoparticles via RAFT alcoholic dispersion polymerisation of BzMA. The progress of this polymerisation was monitored by sampling every 60 min for the first 12 h, see Figure 3. ^{1}H NMR confirmed that 90% conversion was achieved within 12 h (and 94% after 24 h) (Figure 3a). Inspecting the semi-logarithmic plot, three distinct regions can be identified. Initially, there is a linear increase up to 5 h as the initial solution polymerisation of BzMA follows pseudo-first order kinetics. After 5 h, the rate of polymerisation increases by almost a factor of two (1.7), with a second linear regime up to 10 h. In the literature, such behaviour is often explained in terms of micellar nucleation followed by the formation of monomer-swollen copolymer particles, since this leads to a relatively high local monomer concentration [42, 56-59]. However, in the present case, the rate enhancement observed after 5 h does not coincide with the onset of micellisation: TEM studies provide evidence for the

formation of nascent nanoparticles at reaction times as short as 3 h. This discrepancy is not currently understood, but it is worth emphasising that we have recently reported similar observations for other non-aqueous PISA formulations [36, 60]. After 10 h (87% conversion), there is another deviation from linearity in the semi-logarithmic plot as the polymerisation becomes monomer-starved.

DMF GPC analysis during this $PNMEP_{50}$-$PBzMA_{200}$ synthesis indicates a linear increase in M_n with conversion. Relatively low dispersities of less than 1.20 were obtained throughout the BzMA polymerisation, with a final M_w/M_n of 1.17 being obtained after 24 h (94% conversion).

Utilising the above kinetic data, a series of $PNMEP_{50}$-$PBzMA_x$ diblock copolymers were prepared (see Table 1). All syntheses were conducted at 20% w/w solids and allowed to proceed for 24 h at 70 °C. The target PBzMA DP was varied from 50 to 250 and at least 90% conversion was achieved in all cases as judged by ^{1}H NMR spectroscopy. Each diblock copolymer was analysed by DMF GPC (Figure 4). High blocking efficiencies and low dispersities ($M_w/M_n \leq 1.23$) were obtained, indicating the formation of well-defined block copolymers. A gradual shift to lower retention time (higher molecular weight) was observed when targeting higher PBzMA DPs. Thus this RAFT alcoholic dispersion polymerisation formulation is efficient and provides excellent control over the copolymer chains.

Electron microscopy was used to assess the final copolymer morphology, see Figure 5. TEM studies confirmed that spherical micelles were obtained when targeting PBzMA DPs of up to 100. For higher PBzMA DPs, SEM analysis revealed the formation of highly anisotropic worms, with mean worm widths of 96 nm and worm lengths ranging from 1 μm to 6 μm. Compared to the various examples of PBzMA-core worms prepared by RAFT alcoholic dispersion polymerisation reported in the literature,[29, 30] these worms seem to be relatively rod-like, rather than flexible. The reason for this unexpected difference is not understood at the present time. Such dispersions formed brittle turbid gels which proved somewhat difficult to dilute to the relatively low copolymer concentrations required for imaging. Large colloidal aggregates remained after dilution to 0.20% w/w and stirring for 24 h did not overcome this problem. Worm-like clusters were also observed in all cases, see Figure S2. Targeting a PBzMA DP of either 200 or 250 produced polydisperse vesicles of 100 to 500 nm diameter. This change in morphology with increasing PBzMA DP has been reported for many other RAFT dispersion polymerisation formulations in both alcoholic media [29, 30] and *n*-alkanes [21-23].

Synthesis of $PNMEP_{47}$-$PBzMA_{250}$ diblock copolymer nano-objects via a one-pot PISA protocol

Recently, several one-pot protocols have been reported for various PISA formulations [12, 20, 22, 61, 62]. Remarkably good results have been achieved despite adding the second monomer under monomer-starved conditions, which in principle might be expected to compromise RAFT chain-end fidelity. In view of this encouraging literature precedent, the feasibility of a one-pot protocol was examined for the synthesis of PNMEP-PBzMA diblock copolymers.

First, a PNMEP macro-CTA was synthesised at 70 °C by targeting a DP of 50 at 60% w/w solids in ethanol. This RAFT solution homopolymerisation was monitored by ^{1}H NMR spectroscopy. Figure 6a shows the conversion versus time curve and the corresponding semi-logarithmic plot. Very high conversion (97 %) was achieved after 6 h. ^{1}H NMR spectroscopy studies of an aliquot of the macro-CTA solution extracted after 6 h was used to estimate an actual PNMEP DP of 47, which is consistent with the observed monomer conversion within experimental error. This *unpurified* PNMEP macro-CTA was then chain-extended with BzMA at 70 °C, targeting a PBzMA DP of 250 at 30% w/w solids (further ethanol was included as a diluent on addition of the BzMA monomer). The semi-logarithmic plot indicated pseudo-first order kinetics for the entire macro-CTA synthesis, see Figure 6b. A final comonomer conversion of 97% was achieved after 24 h. TEM was used to study the evolution in copolymer morphology during the BzMA polymerisation (see insets shown in Figure 6b). Spherical micelles with a mean diameter of 21 ± 2 nm (based on analysis of more than 50 particles using ImageJ software) were observed after just 1 h. The corresponding monomer conversion (13%) at this time point indicates that a critical PBzMA DP of around 30 is required for micellar nucleation. This is comparable to that reported by Jones et al. for the synthesis of a $PDMA_{31}$-$PBzMA_{37}$ diblock copolymer in ethanol at 70 °C [30]. After 2 h (27% conversion), a mixed phase of predominately worm-like micelles with a few spherical micelles is observed. These worms have a mean thickness of 24 ± 3 nm. Taking experimental error into account, this is comparable to the mean diameter of the original spherical micelles, which suggests that worm formation involves multiple sphere-sphere fusion events. Similar observations have been reported for many other PISA formulations [13-15, 63]. Finally, a pure vesicle phase was observed after 8 h (82% conversion), see Figure S3. This corresponds to a mean PBzMA DP of 205 which is comparable to the DP of 188 required to produce vesicles when using the purified $PNMEP_{50}$ macro-CTA (see entry 8 in Table 1). A pure vesicle phase was also observed after 24 h (97% conversion), when the BzMA polymerisation was terminated.

Both stages of this one-pot PISA formulation were analysed by DMF GPC, see Figure 7. A linear increase in M_n with conversion and a low final dispersity (M_w/M_n = 1.15) were observed for the synthesis of the $PNMEP_{47}$ macro-CTA via RAFT solution polymerisation. The subsequent RAFT dispersion polymerisation of BzMA also resulted in a linear evolution in molecular weight (and a

modest increase in dispersity) with conversion. The final $PNMEP_{47}$-$PBzMA_{243}$ diblock copolymer had an M_n of 23.6 kg mol^{-1} and a dispersity of 1.21 (Figure 8). Apart from a very weak high molecular weight shoulder (which is attributed to a small amount of termination by combination), the unimodal nature of this GPC trace indicates a remarkably high blocking efficiency for the $PNMEP_{47}$ macro-CTA. These data serve to illustrate the potential for utilising highly convenient one-pot synthetic protocols for such PISA formulations.

Conclusions

A series of near-monodisperse $PNMEP_x$ homopolymers were prepared via RAFT solution polymerisation in ethanol at 70 °C. The kinetics of NMEP polymerisation was investigated by systematically varying the CPDB/ACVA molar ratio and the target PNMEP DP. Lowering the CPDB/ACVA molar ratio for $PNMEP_{100}$ from 10.0 to 3.0 led to the final monomer conversion obtained after 24 h increasing from 72% to 98 %. For a constant CTA/ACVA molar ratio of 5.0, increasing the target PNMEP DP reduced the final conversion achieved after 24 h. A linear evolution in molecular weight with conversion was observed in all cases.

A $PNMEP_{50}$ macro-CTA was chain-extended with BzMA at 20% w/w solids via RAFT dispersion polymerisation in ethanol at 70 °C. Kinetic studies indicated that the BzMA polymerisation required 24 h to reach high conversion. A series of $PNMEP_{50}$-$PBzMA_x$ diblocks were prepared in which the target PBzMA DP was varied from 50 to 250 with more than 90% BzMA conversion being achieved in each case. DMF GPC studies indicated a linear relationship between the experimental M_n and the target PBzMA DP, with dispersities below 1.26 being obtained in all cases. Electron microscopy studies confirmed that polymerisation-induced self-assembly occurred during these syntheses, with spherical micelles, worms or vesicles being obtained depending on the target DP of the insoluble PBzMA block.

Finally, a one-pot protocol was examined for the synthesis of a $PNMEP_{47}$-$PBzMA_{243}$ diblock copolymer. ^{1}H NMR analysis indicated that 97 % conversion was achieved for both the RAFT solution polymerisation of NMEP and also the RAFT dispersion polymerisation of BzMA, while GPC studies indicated a relatively low final dispersity of 1.21 for the final diblock copolymer. A gradual evolution in copolymer morphology from spherical micelles to worm-like micelles to vesicles occurred during this one-pot synthesis, as judged by TEM studies.

Acknowledgements

EPSRC is thanked for funding a DTA PhD studentship and also for a Programme Grant (EP/I012060/1). Ashland Specialty Ingredients (Bridgewater, NJ, USA) is thanked for CASE support of this PhD project, for supplying the NMEP monomer and for permission to publish this work.

References

[1] K. Matyjaszewski, N.V. Tsarevsky, Nanostructured functional materials prepared by atom transfer radical polymerization, Nat Chem 1(4) (2009) 276-288.
[2] K. Matyjaszewski, J. Xia, Atom Transfer Radical Polymerization, Chem Rev 101(9) (2001) 2921-2990.
[3] K. Matyjaszewski, Atom transfer radical polymerization (ATRP): current status and future perspectives, Macromolecules 45(10) (2012) 4015-4039.
[4] J. Nicolas, Y. Guillaneuf, C. Lefay, D. Bertin, D. Gigmes, B. Charleux, Nitroxide-mediated polymerization, Progress in Polymer Science 38(1) (2013) 63-235.
[5] R.T.A. Mayadunne, E. Rizzardo, J. Chiefari, Y.K. Chong, G. Moad, S.H. Thang, Living Radical Polymerization with Reversible Addition-Fragmentation Chain Transfer (RAFT Polymerization) Using Dithiocarbamates as Chain Transfer Agents, Macromolecules 32(21) (1999) 6977-6980.
[6] G. Moad, J. Chiefari, Y K. Chong, J. Krstina, R.T.A. Mayadunne, A. Postma, E. Rizzardo, S.H. Thang, Living free radical polymerization with reversible addition - fragmentation chain transfer (the life of RAFT), Polym. Int. 49(9) (2000) 993-1001.
[7] G. Moad, Y.K. Chong, A. Postma, E. Rizzardo, S.H. Thang, Advances in RAFT polymerization: the synthesis of polymers with defined end-groups, Polymer 46(19) (2005) 8458-8468.
[8] G. Moad, E. Rizzardo, S.H. Thang, Living radical polymerization by the RAFT process, Australian Journal of Chemistry 58(6) (2005) 379-410.
[9] G. Moad, E. Rizzardo, S.H. Thang, Living Radical Polymerization by the RAFT Process—A First Update, Australian Journal of Chemistry 59(10) (2006) 669-692.
[10] G. Moad, E. Rizzardo, S.H. Thang, Toward Living Radical Polymerization, Accounts of Chemical Research 41(9) (2008) 1133-1142.
[11] G. Moad, E. Rizzardo, S.H. Thang, Living radical polymerization by the RAFT process–a second update, Australian Journal of Chemistry 62(11) (2009) 1402-1472.
[12] B. Charleux, G. Delaittre, J. Rieger, F. D'Agosto, Polymerization-Induced Self-Assembly: From Soluble Macromolecules to Block Copolymer Nano-Objects in One Step, Macromolecules 45 (2012) 6753-6765.
[13] N.J. Warren, S.P. Armes, Polymerization-Induced Self-Assembly of Block Copolymer Nano-objects via RAFT Aqueous Dispersion Polymerization, Journal of the American Chemical Society 136(29) (2014) 10174-10185.
[14] M.J. Derry, L.A. Fielding, S.P. Armes, Polymerization-induced self-assembly of block copolymer nanoparticles via RAFT non-aqueous dispersion polymerization, Progress in Polymer Science 52 (2016) 1-18.
[15] S.L. Canning, G.N. Smith, S.P. Armes, A Critical Appraisal of RAFT-Mediated Polymerization-Induced Self-Assembly, Macromolecules 49(6) (2016) 1985-2001.
[16] Y. Li, S.P. Armes, RAFT Synthesis of Sterically Stabilized Methacrylic Nanolatexes and Vesicles by Aqueous Dispersion Polymerization, Angewandte Chemie International Edition 49(24) (2010) 4042-4046.
[17] C.L. McCormick, A.B. Lowe, Aqueous RAFT Polymerization: Recent Developments in Synthesis of Functional Water-Soluble (Co)polymers with Controlled Structures†, Accounts of Chemical Research 37(5) (2004) 312-325.
[18] A. Blanazs, A.J. Ryan, S.P. Armes, Predictive Phase Diagrams for RAFT Aqueous Dispersion Polymerization: Effect of Block Copolymer Composition, Molecular Weight, and Copolymer Concentration, Macromolecules 45(12) (2012) 5099-5107.

[19] N.J. Warren, O.O. Mykhaylyk, D. Mahmood, A.J. Ryan, S.P. Armes, RAFT Aqueous Dispersion Polymerization Yields Poly(ethylene glycol)-Based Diblock Copolymer Nano-Objects with Predictable Single Phase Morphologies, Journal of the American Chemical Society 136(3) (2014) 1023-1033.
[20] L.P.D. Ratcliffe, A.J. Ryan, S.P. Armes, From a Water-Immiscible Monomer to Block Copolymer Nano-Objects via a One-Pot RAFT Aqueous Dispersion Polymerization Formulation, Macromolecules 46(3) (2013) 769-777.
[21] L.A. Fielding, M.J. Derry, V. Ladmiral, J. Rosselgong, A.M. Rodrigues, L.P. Ratcliffe, S. Sugihara, S.P. Armes, RAFT dispersion polymerization in non-polar solvents: facile production of block copolymer spheres, worms and vesicles in n-alkanes, Chemical Science 4(5) (2013) 2081-2087.
[22] M.J. Derry, L.A. Fielding, S.P. Armes, Industrially-relevant polymerization-induced self-assembly formulations in non-polar solvents: RAFT dispersion polymerization of benzyl methacrylate, Polymer Chemistry 6(16) (2015) 3054-3062.
[23] L.A. Fielding, J.A. Lane, M.J. Derry, O.O. Mykhaylyk, S.P. Armes, Thermo-responsive Diblock Copolymer Worm gels in Non-polar Solvents, Journal of the American Chemical Society 136(15) (2014) 5790-5798.
[24] L. Houillot, C. Bui, C. Farcet, C. Moire, J.-A. Raust, H. Pasch, M. Save, B. Charleux, Dispersion Polymerization of Methyl Acrylate in Nonpolar Solvent Stabilized by Block Copolymers Formed In situ via the RAFT Process, Acs Applied Materials & Interfaces 2(2) (2010) 434-442.
[25] L. Houillot, C. Bui, M. Save, B. Charleux, C. Farcet, C. Moire, J.-A. Raust, I. Rodriguez, Synthesis of well-defined polyacrylate particle dispersions in organic medium using simultaneous RAFT polymerization and self-assembly of block copolymers. A strong influence of the selected thiocarbonylthio chain transfer agent, Macromolecules 40(18) (2007) 6500-6509.
[26] Y. Pei, O.R. Sugita, L. Thurairajah, A.B. Lowe, Synthesis of poly (stearyl methacrylate-b-3-phenylpropyl methacrylate) nanoparticles in n-octane and associated thermoreversible polymorphism, RSC Advances 5(23) (2015) 17636-17646.
[27] Y. Pei, L. Thurairajah, O.R. Sugita, A.B. Lowe, RAFT Dispersion Polymerization in Nonpolar Media: Polymerization of 3-Phenylpropyl Methacrylate in n-Tetradecane with Poly(stearyl methacrylate) Homopolymers as Macro Chain Transfer Agents, Macromolecules 48(1) (2015) 236-244.
[28] G. Johnston-Hall, J.R. Harjani, P.J. Scammells, M.J. Monteiro, RAFT-Mediated Polymerization of Styrene in Readily Biodegradable Ionic Liquids, Macromolecules 42(5) (2009) 1604-1609.
[29] M. Semsarilar, E.R. Jones, A. Blanazs, S.P. Armes, Efficient Synthesis of Sterically-Stabilized Nano-Objects via RAFT Dispersion Polymerization of Benzyl Methacrylate in Alcoholic Media Advanced Materials 24 (2012) 3378-3382.
[30] E.R. Jones, M. Semsarilar, A. Blanazs, S.P. Armes, Efficient Synthesis of Amine-Functional Diblock Copolymer Nanoparticles via RAFT Dispersion Polymerization of Benzyl Methacrylate in Alcoholic Media, Macromolecules 45(12) (2012) 5091-5098.
[31] W. Zhao, G. Gody, S. Dong, P.B. Zetterlund, S. Perrier, Optimization of the RAFT polymerization conditions for the in situ formation of nano-objects via dispersion polymerization in alcoholic medium, Polymer Chemistry 5(24) (2014) 6990-7003.
[32] Y. Pei, A.B. Lowe, Polymerization-induced self-assembly: ethanolic RAFT dispersion polymerization of 2-phenylethyl methacrylate, Polymer Chemistry 5(7) (2014) 2342-2351.
[33] M. Semsarilar, V. Ladmiral, A. Blanazs, S.P. Armes, Poly (methacrylic acid)-based AB and ABC block copolymer nano-objects prepared via RAFT alcoholic dispersion polymerization, Polymer Chemistry 5(10) (2014) 3466-3475.
[34] Y. Pei, N.C. Dharsana, J.A. van Hensbergen, R.P. Burford, P.J. Roth, A.B. Lowe, RAFT dispersion polymerization of 3-phenylpropyl methacrylate with poly[2-(dimethylamino)ethyl methacrylate] macro-CTAs in ethanol and associated thermoreversible polymorphism, Soft Matter 10(31) (2014) 5787-5796.
[35] M. Semsarilar, N.J. Penfold, E.R. Jones, S.P. Armes, Semi-crystalline diblock copolymer nano-objects prepared via RAFT alcoholic dispersion polymerization of stearyl methacrylate, Polymer Chemistry 6(10) (2015) 1751-1757.

[36] E.R. Jones, M. Semsarilar, P. Wyman, M. Boerakker, S.P. Armes, Addition of water to an alcoholic RAFT PISA formulation leads to faster kinetics but limits the evolution of copolymer morphology, Polymer Chemistry (7) (2016) 851.
[37] W. Cai, W. Wan, C. Hong, C. Huang, C.-Y. Pan, Morphology transitions in RAFT polymerization, Soft Matter 6(21) (2010) 5554-5561.
[38] C.-Q. Huang, C.-Y. Pan, Direct preparation of vesicles from one-pot RAFT dispersion polymerization, Polymer 51(22) (2010) 5115-5121.
[39] W.M. Wan, X.L. Sun, C.Y. Pan, Formation of Vesicular Morphologies via Polymerization Induced Self-Assembly and Re-Organization, Macromolecular Rapid Communications 31(4) (2010) 399-404.
[40] W.-M. Wan, C.-Y. Pan, Formation of polymeric yolk/shell nanomaterial by polymerization-induced self-assembly and reorganization, Macromolecules 43(6) (2010) 2672-2675.
[41] X. Zhang, J. Rieger, B. Charleux, Effect of the solvent composition on the morphology of nano-objects synthesized via RAFT polymerization of benzyl methacrylate in dispersed systems, Polymer Chemistry (2012) 1502-1509.
[42] M. Semsarilar, V. Ladmiral, A. Blanazs, S.P. Armes, Anionic Polyelectrolyte-Stabilized Nanoparticles via RAFT Aqueous Dispersion Polymerization, Langmuir 28(1) (2012) 914-922.
[43] X. Wang, J. Xu, Y. Zhang, W. Zhang, Polymerization of styrene in alcohol/water mediated by a macro-RAFT agent of poly(N-isopropylacrylamide) trithiocarbonate: From homogeneous to heterogeneous RAFT polymerization, Journal of Polymer Science Part A: Polymer Chemistry 50(12) (2012) 2452-2462.
[44] F. Huo, X. Wang, Y. Zhang, X. Zhang, J. Xu, W. Zhang, RAFT Dispersion Polymerization of Styrene in Water/Alcohol: The Solvent Effect on Polymer Particle Growth during Polymer Chain Propagation, Macromolecular Chemistry and Physics 214(8) (2013) 902-911.
[45] J. Deng, Y. Shi, W. Jiang, Y. Peng, L. Lu, Y. Cai, Facile synthesis and thermoresponsive behaviors of a well-defined pyrrolidone based hydrophilic polymer, Macromolecules 41(9) (2008) 3007-3014.
[46] J. Sun, Y. Peng, Y. Chen, Y. Liu, J. Deng, L. Lu, Y. Cai, Effect of Molecular Structure on Thermoresponsive Behaviors of Pyrrolidone-Based Water-Soluble Polymers, Macromolecules 43(9) (2010) 4041-4049.
[47] J. Zhang, M. Zou, J. Dong, X. Li, Synthesis and self-assembly behaviors of well-defined poly (lauryl methacrylate)-block-poly [N-(2-methacryloylxyethyl) pyrrolidone] copolymers, Colloid and Polymer Science 291(11) (2013) 2653-2662.
[48] V.J. Cunningham, S.P. Armes, O.M. Musa, Synthesis, characterisation and Pickering emulsifier performance of poly(stearyl methacrylate)-poly(N-2-(methacryloyloxy)ethyl pyrrolidone) diblock copolymer nano-objects via RAFT dispersion polymerisation in n-dodecane, Polymer Chemistry 7(10) (2016) 1882-1891.
[49] G. Pound, Z. Eksteen, R. Pfukwa, J.M. McKenzie, R.F. Lange, B. Klumperman, Unexpected reactions associated with the xanthate-mediated polymerization of N-vinylpyrrolidone, Journal of Polymer Science Part A: Polymer Chemistry 46(19) (2008) 6575-6593.
[50] I.J. Johnson, Khosravi, E., Musa, O. M., Simnett, R. E. and Eissa, A. M., Xanthates designed for the preparation of N-Vinyl pyrrolidone-based linear and star architectures via RAFT polymerization, J. Polym. Sci. Part A: Polym. Chem. 53 (2015) 775-786.
[51] N. Bailly, G. Pound-Lana, B. Klumperman, Synthesis, Characterization, and Self-Assembly of Poly (N-vinylpyrrolidone)-block-poly (vinyl acetate), Australian Journal of Chemistry 65(8) (2012) 1124-1131.
[52] N. Bailly, M. Thomas, B. Klumperman, Poly (N-vinylpyrrolidone)-block-poly (vinyl acetate) as a Drug Delivery Vehicle for Hydrophobic Drugs, Biomacromolecules 13(12) (2012) 4109-4117.
[53] M. Destarac, Controlled Radical Polymerization: Industrial Stakes, Obstacles and Achievements, Macromolecular Reaction Engineering 4(3-4) (2010) 165-179.
[54] A. Guinaudeau, O. Coutelier, A. Sandeau, S. Mazières, H.D. Nguyen Thi, V. Le Drogo, D.J. Wilson, M. Destarac, Facile Access to Poly (N-vinylpyrrolidone)-Based Double Hydrophilic Block Copolymers by Aqueous Ambient RAFT/MADIX Polymerization, Macromolecules 47(1) (2013) 41-50.

[55] J. Rieger, Guidelines for the Synthesis of Block Copolymer Particles of Various Morphologies by RAFT Dispersion Polymerization, Macromolecular Rapid Communications 36(16) (2015) 1458-1471.
[56] A. Blanazs, J. Madsen, G. Battaglia, A.J. Ryan, S.P. Armes, Mechanistic Insights for Block Copolymer Morphologies: How Do Worms Form Vesicles?, Journal of the American Chemical Society 133(41) (2011) 16581-16587.
[57] M. Semsarilar, V. Ladmiral, A. Blanazs, S.P. Armes, Cationic Polyelectrolyte-Stabilized Nanoparticles via RAFT Aqueous Dispersion Polymerization, Langmuir 29(24) (2013) 7416-7424.
[58] X. Xiao, S. He, M. Dan, Y. Su, F. Huo, W. Zhang, Brush macro-RAFT agent mediated dispersion polymerization of styrene in the alcohol/water mixture, Journal of Polymer Science Part A: Polymer Chemistry 51(15) (2013) 3177-3190.
[59] Y. Su, X. Xiao, S. Li, M. Dan, X. Wang, W. Zhang, Precise evaluation of the block copolymer nanoparticle growth in polymerization-induced self-assembly under dispersion conditions, Polymer Chemistry 5(2) (2014) 578-587.
[60] A.P. Lopez-Oliva, N.J. Warren, A. Rajkumar, O.O. Mykhaylyk, M.J. Derry, K.E. Doncom, M.J. Rymaruk, S.P. Armes, Polydimethylsiloxane-Based Diblock Copolymer Nano-objects Prepared in Nonpolar Media via RAFT-Mediated Polymerization-Induced Self-Assembly, Macromolecules 48(11) (2015) 3547-3555.
[61] W. Zhang, F. D'Agosto, O. Boyron, J. Rieger, B. Charleux, One-Pot Synthesis of Poly(methacrylic acid-co-poly(ethylene oxide) methyl ether methacrylate)-b-polystyrene Amphiphilic Block Copolymers and Their Self-Assemblies in Water via RAFT-Mediated Radical Emulsion Polymerization. A Kinetic Study, Macromolecules 44(19) (2011) 7584-7593.
[62] W. Zhang, F. D'Agosto, P.-Y. Dugas, J. Rieger, B. Charleux, RAFT-mediated one-pot aqueous emulsion polymerization of methyl methacrylate in presence of poly(methacrylic acid-co-poly(ethylene oxide) methacrylate) trithiocarbonate macromolecular chain transfer agent, Polymer 54(8) (2013) 2011-2019.
[63] K.E. Doncom, N.J. Warren, S.P. Armes, Polysulfobetaine-based diblock copolymer nano-objects via polymerization-induced self-assembly, Polymer Chemistry 6(41) (2015) 7264-7273.

List of Tables

Table 1. Conversions, Solids Content, Molecular Weights (M_n), Dispersities (M_w/M_n), Mean Particle Diameter and Morphology obtained for $PNMEP_{50}$-$PBzMA_x$ Diblock Copolymer Nanoparticles and the corresponding $PNMEP_{50}$ Macro-CTA. (N.B. 'N' denotes PNMEP and 'B' denotes PBzMA)

Table 1. Conversions, Solids Content, Molecular Weights (M_n), Dispersities (M_w/M_n), Mean Particle Diameter and Morphology obtained for $PNMEP_{50}$-$PBzMA_x$ Diblock Copolymer Nanoparticles and the corresponding $PNMEP_{50}$ Macro-CTA. (N.B. 'N' denotes PNMEP and 'B' denotes PBzMA)

	Diblock Composition	Conversion[a] (%)	Solids content (% w/w)	DMF GPC		Morphology
				M_n [b] (g mol^{-1})	M_w/M_n [b]	
1	N_{50}	91	60	8,000	1.15	-
2	N_{50}-B_{47}	94	20	12,000	1.20	Spheres[d]
3	N_{50}-B_{69}	93	20	13,100	1.20	Spheres[d]
4	N_{50}-B_{94}	94	20	14,400	1.21	Spheres[d] (+ short worms)
5	N_{50}-B_{115}	94	20	16,400	1.21	Worms[e]
6	N_{50}-B_{144}	96	20	17,900	1.24	Worms[e]
7	N_{50}-B_{158}	90	20	19,700	1.20	Worms[e] (+ vesicles)
8	N_{50}-B_{188}	94	20	21,200	1.23	Vesicles[d]
9	N_{50}-B_{233}	93	20	24,100	1.25	Vesicles[d]

a. Conversion determined by ^{1}H NMR spectroscopy in d-chloroform except for entry 1 where d_4-methanol was used

b. Determined by DMF GPC against poly(methyl methacrylate) calibration standards

c. The number in brackets refers to the DLS polydispersity of the sample

d. Determined by TEM

e. Determined by SEM

List of Schemes

Scheme 1. Synthesis of PNMEP homopolymers via RAFT solution polymerisation at 70 °C.

Scheme 2. The preparation of $PNMEP_{50}$-$PBzMA_x$ diblock copolymers via RAFT alcoholic dispersion polymerisation at 70 °C, these diblock copolymers undergo PISA to form spherical micelles, worm-like micelles and vesicles.

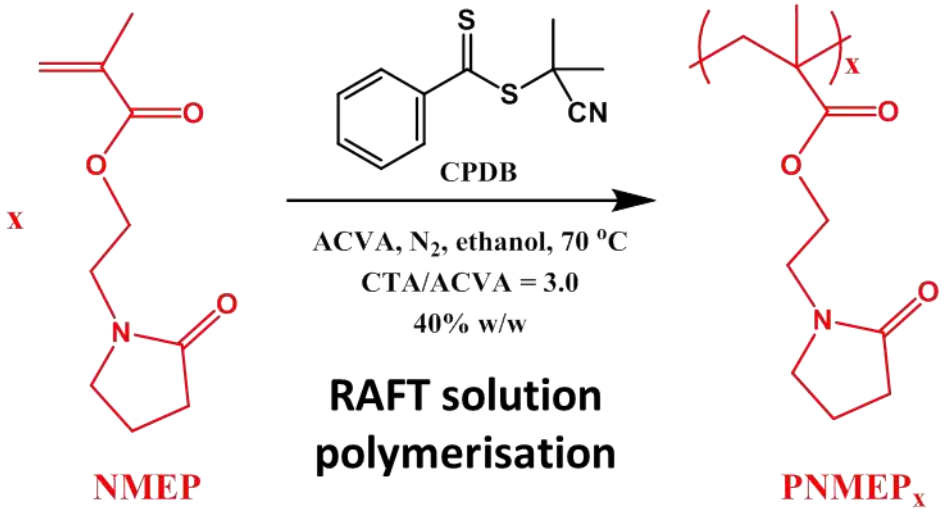

Scheme 1. Synthesis of PNMEP homopolymers via RAFT solution polymerisation at 70 °C.

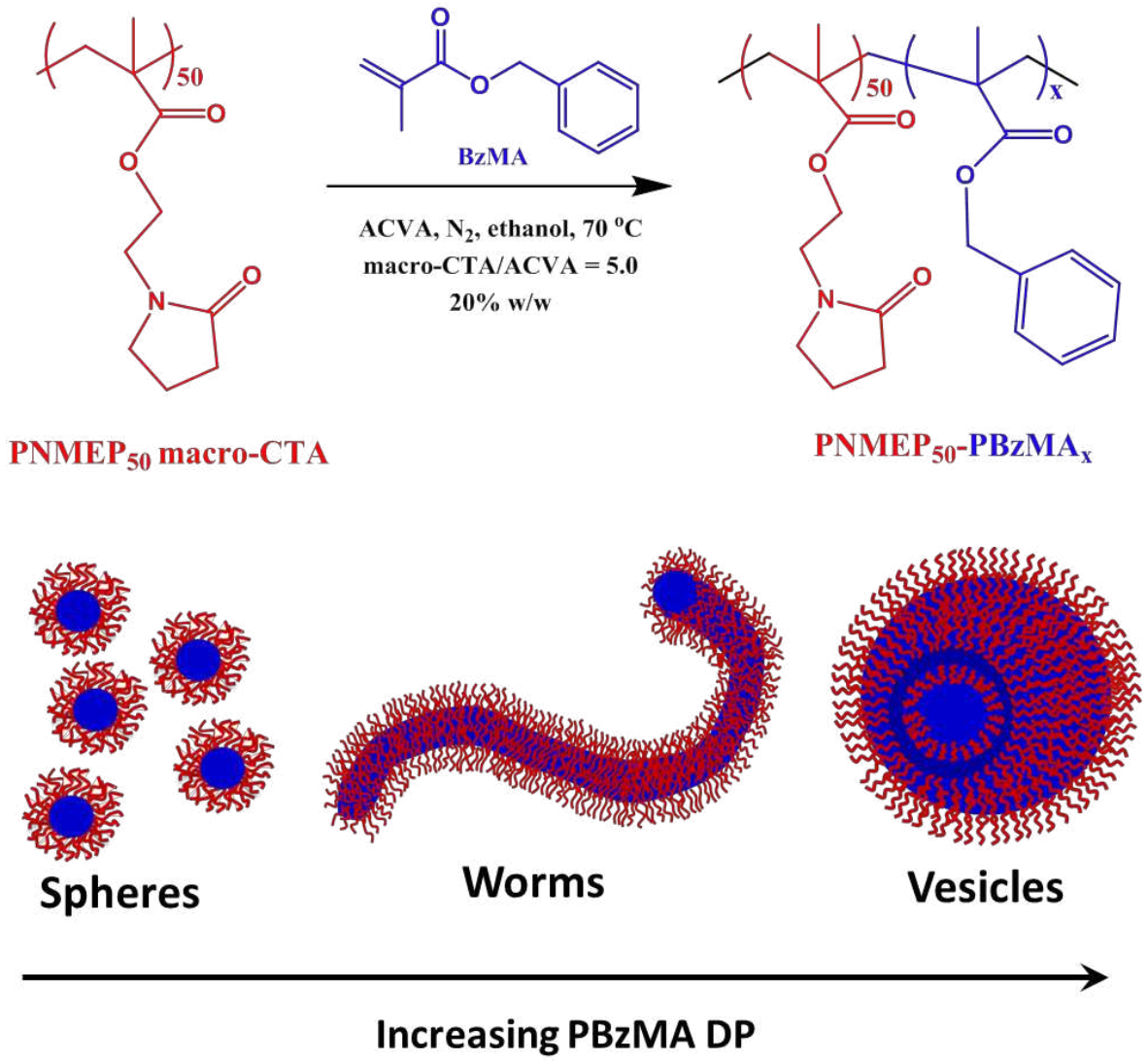

Scheme 2. The preparation of $PNMEP_{50}$-$PBzMA_x$ diblock copolymers via RAFT alcoholic dispersion polymerisation at 70 °C, these diblock copolymers undergo PISA to form spherical micelles, worm-like micelles and vesicles.

List of Figures

Figure 1. Kinetics of the RAFT solution polymerisation of NMEP in ethanol at 70 °C at an $[NMEP]_o$ of 40% w/w solids. (a) Conversion vs. time curves and (b) corresponding semi-logarithmic plots obtained when targeting $PNMEP_{100}$ using CPDB/ACVA molar ratios of 3.0, 5.0, 7.0 and 10.0. Pseudo-first order rate constants calculated for the initial linear regimes are 1.08×10^{-4} s^{-1} (3.0), 7.42×10^{-5} s^{-1} (5.0), 4.94×10^{-5} s^{-1} (7.0) and 3.48×10^{-5} (10.0), where the numbers in brackets refer to the CPBD/ACVA molar ratio in each case.

Figure 2. (a) Conversion versus time plot obtained for the RAFT solution polymerisation of NMEP at 70 °C for a CPDB/ACVA molar ratio of 5.0 at $[NMEP]_o$ = 40% w/w targeting a PBzMA DP (x) of 70, 100, 200 or 400. (b) Corresponding M_n vs. conversion plots for $PNMEP_{70}$, $PNMEP_{100}$, $PNMEP_{200}$ and $PNMEP_{400}$ (DMF eluent; refractive index detector; calibrated using a series of near-monodisperse poly(methyl methacrylate) standards).

Figure 3. Kinetic and GPC data obtained during the RAFT alcoholic dispersion polymerisation of BzMA at 70 °C targeting $PNMEP_{50}$-$PBzMA_{200}$ at 20% w/w solids using a macro-CTA/ACVA molar ratio of 5.0: (a) conversion vs. time curves and corresponding semi-logarithmic plots as determined by ^1H NMR analysis in $CDCl_3$; (b) evolution of M_n (blue axis) and M_w/M_n (red axis) with conversion (DMF eluent; refractive index detector; calibration using a series of near-monodisperse poly(methyl methacrylate) standards).

Figure 4. DMF GPC chromatograms obtained for a series of $PNMEP_{50}$-$PBzMA_x$ diblock copolymers prepared at 20% w/w solids via RAFT alcoholic dispersion polymerisation of BzMA at 70 °C (N.B. for brevity, 'N' denotes PNMEP and 'B' denotes PBzMA).

Figure 5. Electron microscopy images obtained for (a) $PNMEP_{50}$-$PBzMA_{69}$, (b) $PNMEP_{50}$-$PBzMA_{146}$ and (c) $PNMEP_{50}$-$PBzMA_{188}$ nano-objects prepared via RAFT dispersion polymerisation of BzMA at 70 ^oC in ethanol at 20% w/w solids. The mean PBzMA DP dictates the formation of spherical micelles, highly anisotropic worms and vesicles, respectively.

Figure 6. Kinetic data obtained for the one-pot synthesis of $PNMEP_{47}$-$PBzMA_{243}$ diblock copolymer vesicles. (a) RAFT solution polymerisation of a $PNMEP_{47}$ macro-CTA at 60% w/w in ethanol at 70 °C, (b) RAFT alcoholic dispersion polymerisation of BzMA using this unpurified $PNMEP_{47}$ macro-CTA at 30% w/w solids at 70 °C in ethanol. Inset: representative TEM images obtained for the growing $PNMEP_{47}$-$PBzMA_{250}$ nano-objects after 1 h (13% BzMA conversion), 2 h (27% BzMA) and 24 h (97% BzMA).

Figure 7. DMF GPC data obtained during the one-pot synthesis of $PNMEP_{47}$-$PBzMA_{243}$ vesicles at 70 °C using a CTA/initiator molar ratio of 3.0. (a) Synthesis of $PNMEP_{47}$ macro-CTA via RAFT solution polymerisation of NMEP at 60% w/w solids. (b) Synthesis of $PNMEP_{47}$-$PBzMA_{243}$ diblock copolymer vesicles via RAFT alcoholic dispersion polymerisation of BzMA at 30% w/w solids. (Refractive index detector, vs. a series of near-monodisperse poly(methyl methacrylate) calibration standards).

Figure 8. GPC analysis of the one-pot synthesis of $PNMEP_{47}$-$PBzMA_{243}$ at 70 °C. The black trace shows the $PNMEP_{47}$ macro-CTA after 6 h (97% conversion for an aliquot taken just before BzMA addition) synthesised using a CTA/initiator molar ratio of 3.0 at 60% w/w solids. The blue trace shows the $PNMEP_{47}$-$PBzMA_{243}$ diblock copolymer obtained after 24 h using a macro-CTA/initiator molar ratio of 5.0 at 30% w/w solids. (DMF eluent; refractive index detector; calibration using a series of near-monodisperse poly(methyl methacrylate) standards).

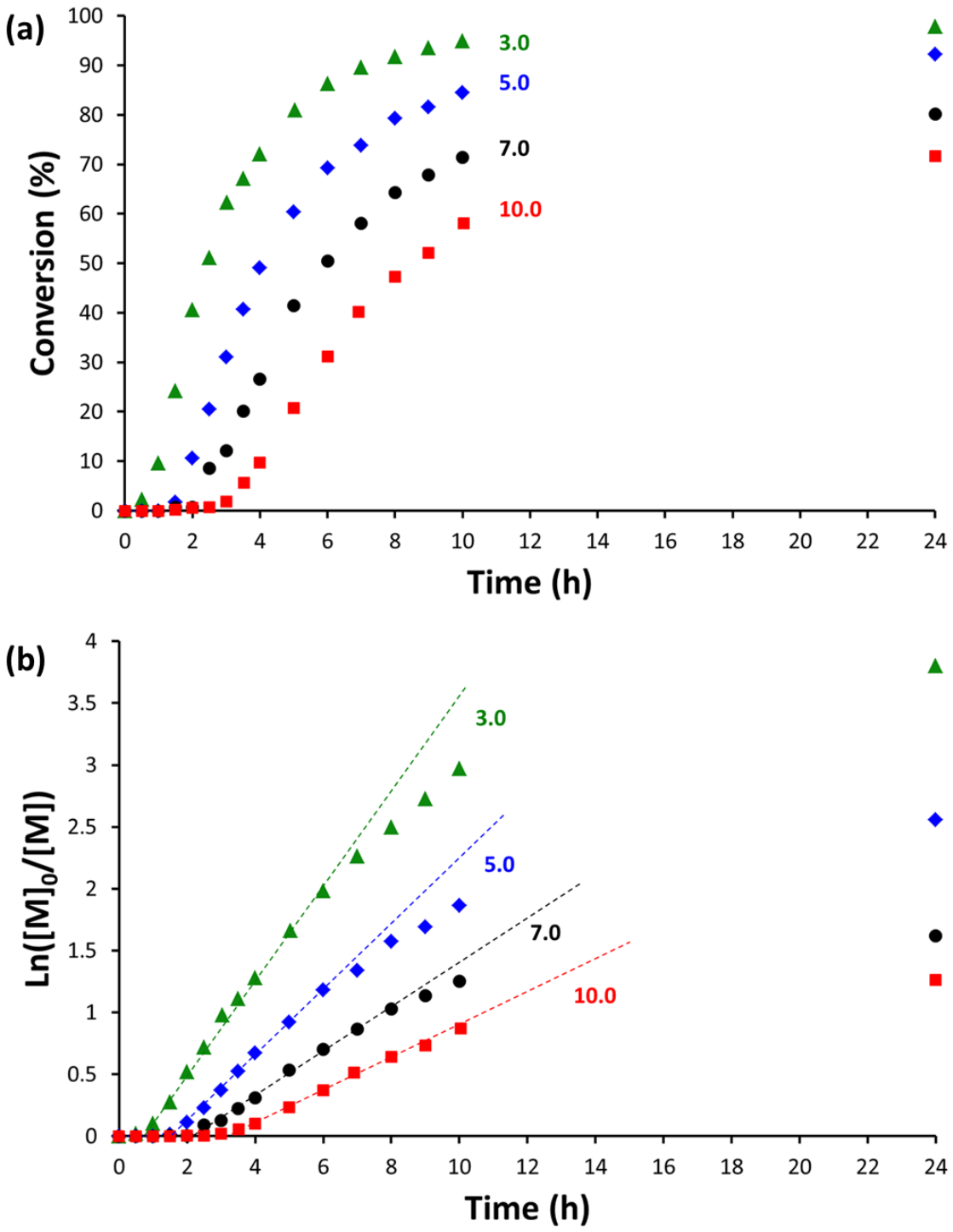

Figure 1. Kinetics of the RAFT solution polymerisation of NMEP in ethanol at 70 °C at an $[NMEP]_o$ of 40% w/w solids. (a) Conversion vs. time curves and (b) corresponding semi-logarithmic plots obtained when targeting $PNMEP_{100}$ using CPDB/ACVA molar ratios of 3.0, 5.0, 7.0 and 10.0. Pseudo-first order rate constants calculated for the initial linear regimes are 1.08 x 10^{-4} s^{-1} (3.0), 7.42 x 10^{-5} s^{-1} (5.0), 4.94 x 10^{-5} s^{-1} (7.0) and 3.48 x 10^{-5} (10.0), where the numbers in brackets refer to the CPBD/ACVA molar ratio in each case.

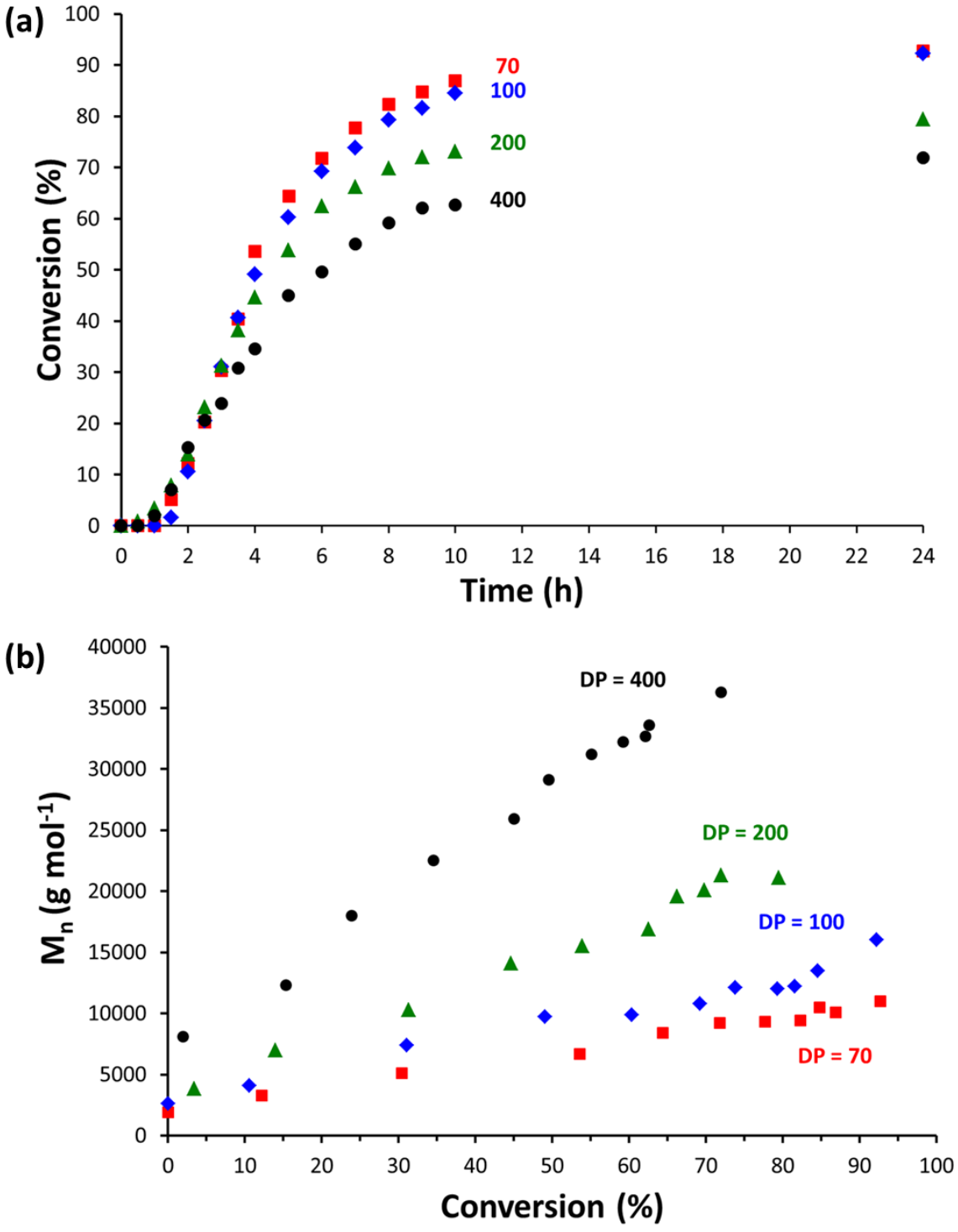

Figure 2. (a) Conversion versus time plot obtained for the RAFT solution polymerisation of NMEP at 70 °C for a CPDB/ACVA molar ratio of 5.0 at $[NMEP]_o$ = 40% w/w targeting a PBzMA DP (x) of 70, 100, 200 or 400. (b) Corresponding M_n vs. conversion plots for $PNMEP_{70}$, $PNMEP_{100}$, $PNMEP_{200}$ and $PNMEP_{400}$ (DMF eluent; refractive index detector; calibrated using a series of near-monodisperse poly(methyl methacrylate) standards).

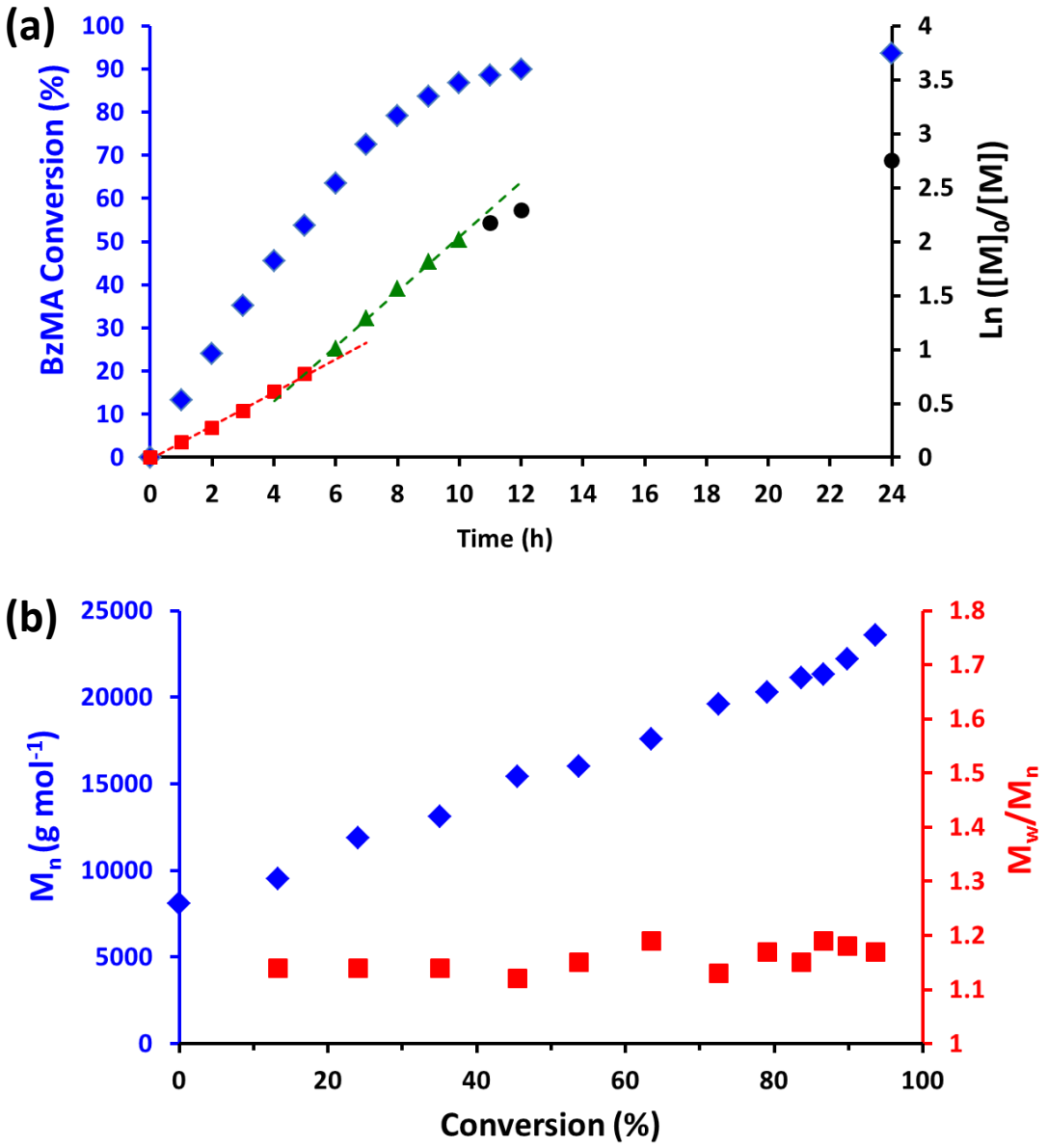

Figure 3. Kinetic and GPC data obtained during the RAFT alcoholic dispersion polymerisation of BzMA at 70 °C targeting $PNMEP_{50}$-$PBzMA_{200}$ at 20% w/w solids using a macro-CTA/ACVA molar ratio of 5.0: (a) conversion vs. time curves and corresponding semi-logarithmic plots as determined by ^1H NMR analysis in $CDCl_3$; (b) evolution of M_n (blue axis) and M_w/M_n (red axis) with conversion (DMF eluent; refractive index detector; calibration using a series of near-monodisperse poly(methyl methacrylate) standards).

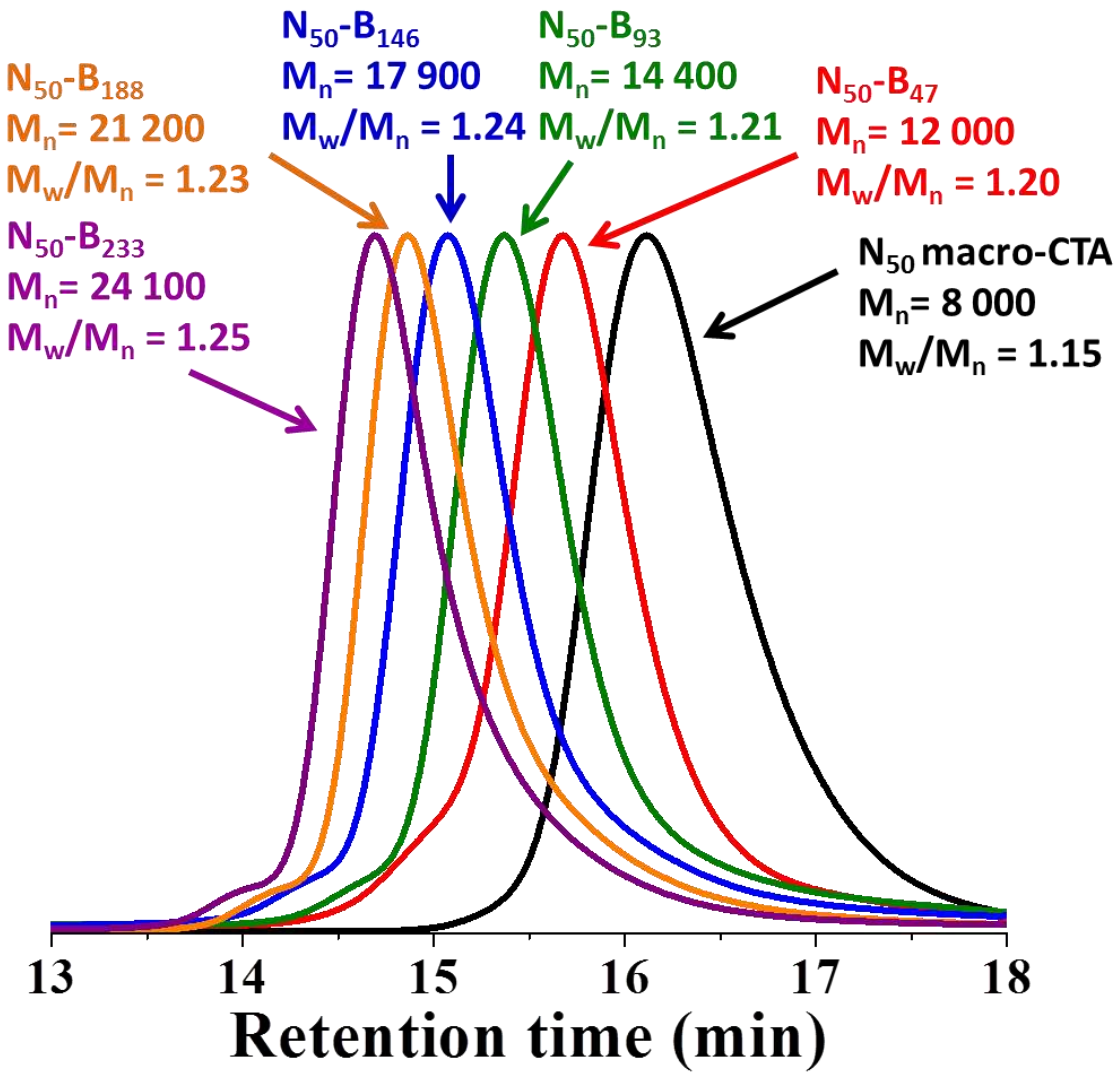

Figure 4. DMF GPC chromatograms obtained for a series of $PNMEP_{50}$-$PBzMA_x$ diblock copolymers prepared at 20% w/w solids via RAFT alcoholic dispersion polymerisation of BzMA at 70 °C (N.B. for brevity, 'N' denotes PNMEP and 'B' denotes PBzMA).

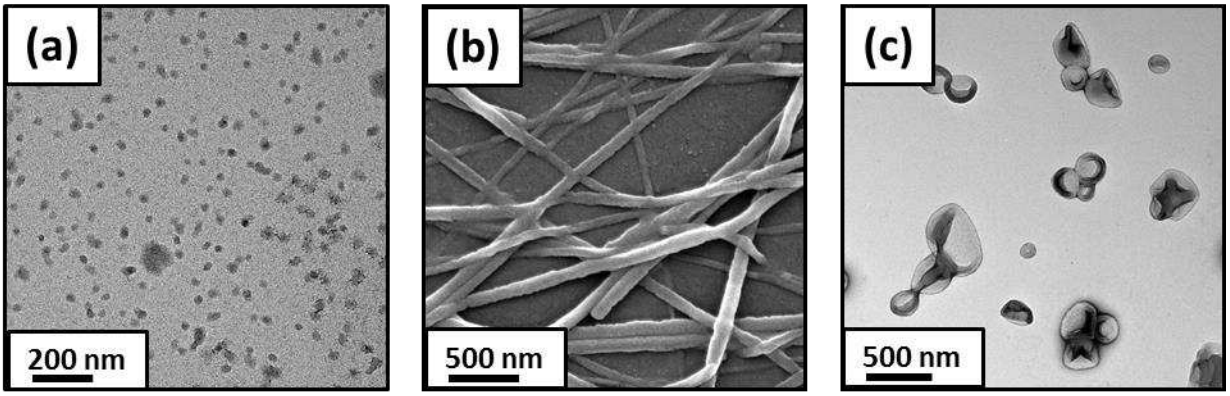

Figure 5. Electron microscopy images obtained for (a) $PNMEP_{50}$-$PBzMA_{69}$, (b) $PNMEP_{50}$-$PBzMA_{146}$ and (c) $PNMEP_{50}$-$PBzMA_{188}$ nano-objects prepared via RAFT dispersion polymerisation of BzMA at 70 ^{o}C in ethanol at 20% w/w solids. The mean PBzMA DP dictates the formation of spherical micelles, highly anisotropic worms and vesicles, respectively.

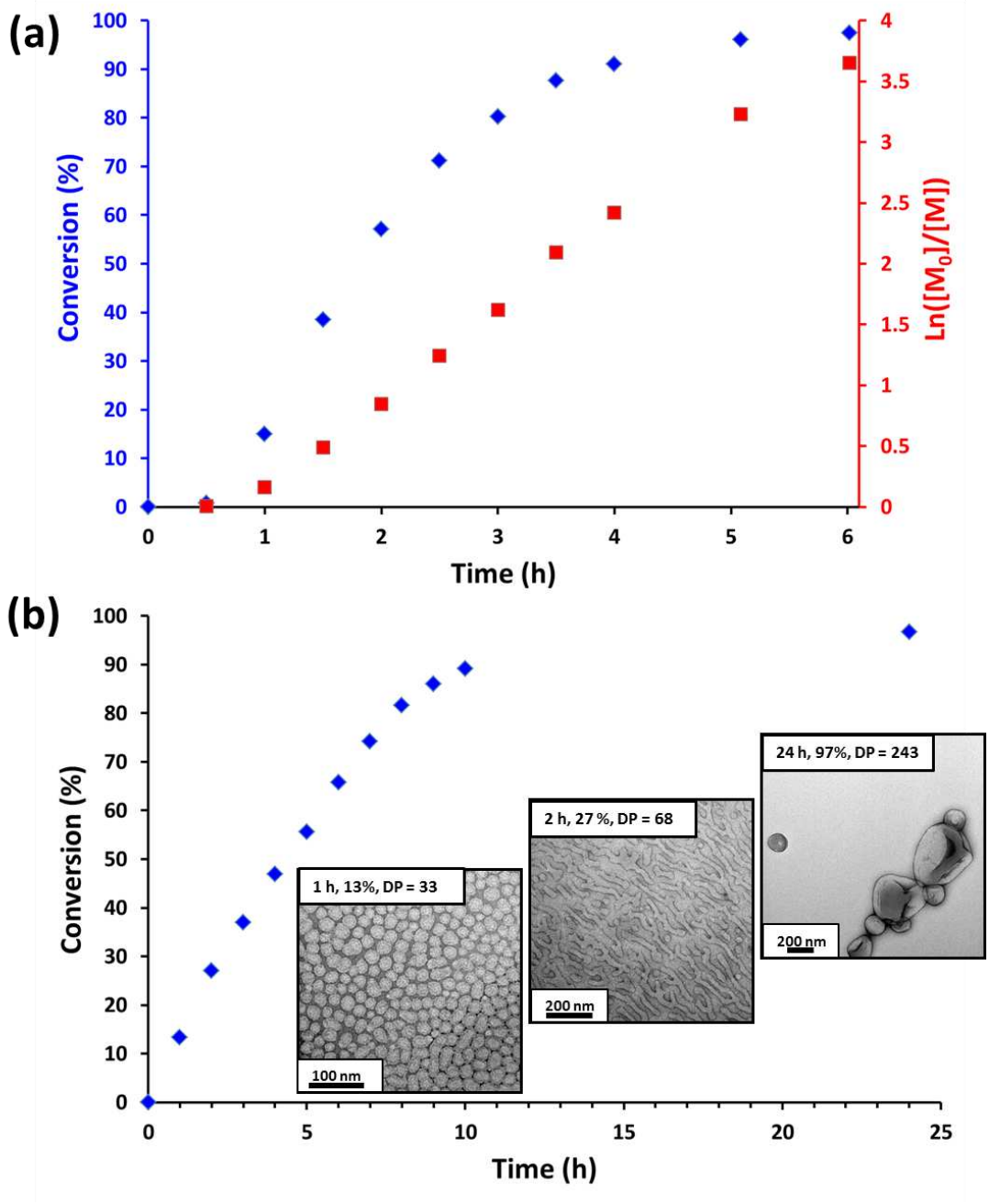

Figure 6. Kinetic data obtained for the one-pot synthesis of $PNMEP_{47}$-$PBzMA_{243}$ diblock copolymer vesicles. (a) RAFT solution polymerisation of a $PNMEP_{47}$ macro-CTA at 60% w/w in ethanol at 70 °C, (b) RAFT alcoholic dispersion polymerisation of BzMA using this unpurified $PNMEP_{47}$ macro-CTA at 30% w/w solids at 70 °C in ethanol. Inset: representative TEM images obtained for the growing $PNMEP_{47}$-$PBzMA_{250}$ nano-objects after 1 h (13% BzMA conversion), 2 h (27% BzMA) and 24 h (97% BzMA).

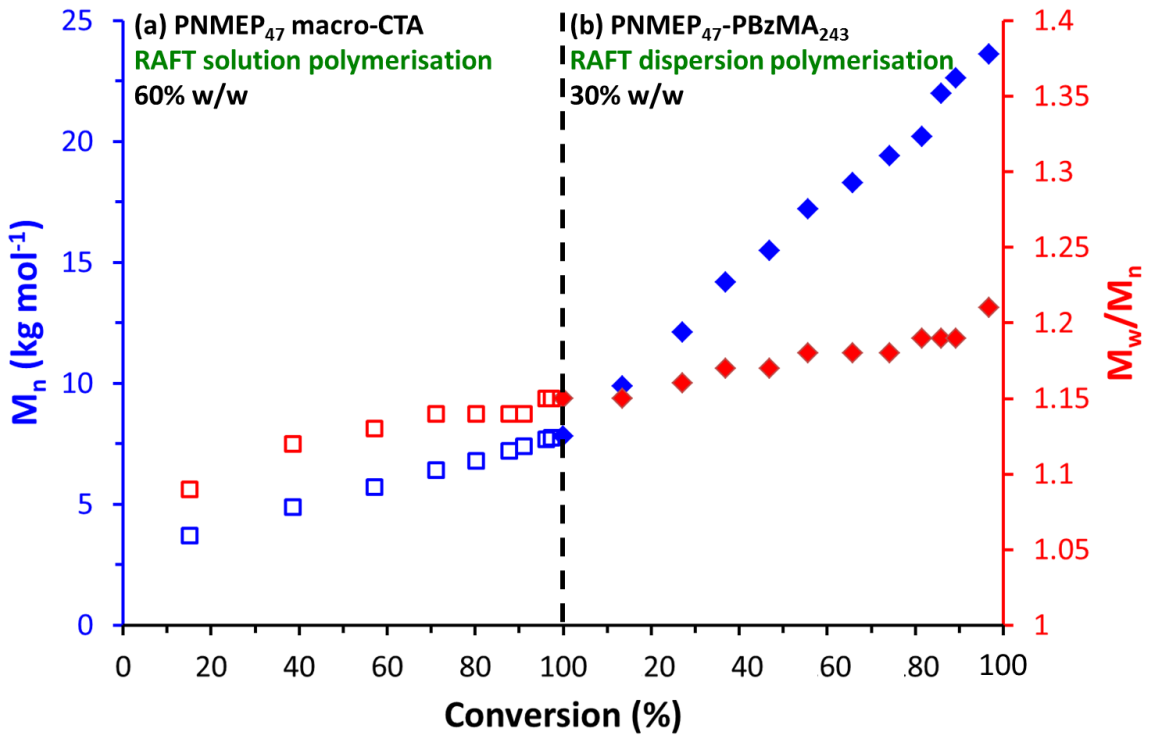

Figure 7. DMF GPC data obtained during the one-pot synthesis of $PNMEP_{47}$-$PBzMA_{243}$ vesicles at 70 °C using a CTA/initiator molar ratio of 3.0. (a) Synthesis of $PNMEP_{47}$ macro-CTA via RAFT solution polymerisation of NMEP at 60% w/w solids. (b) Synthesis of $PNMEP_{47}$-$PBzMA_{243}$ diblock copolymer vesicles via RAFT alcoholic dispersion polymerisation of BzMA at 30% w/w solids. (Refractive index detector, vs. a series of near-monodisperse poly(methyl methacrylate) calibration standards).

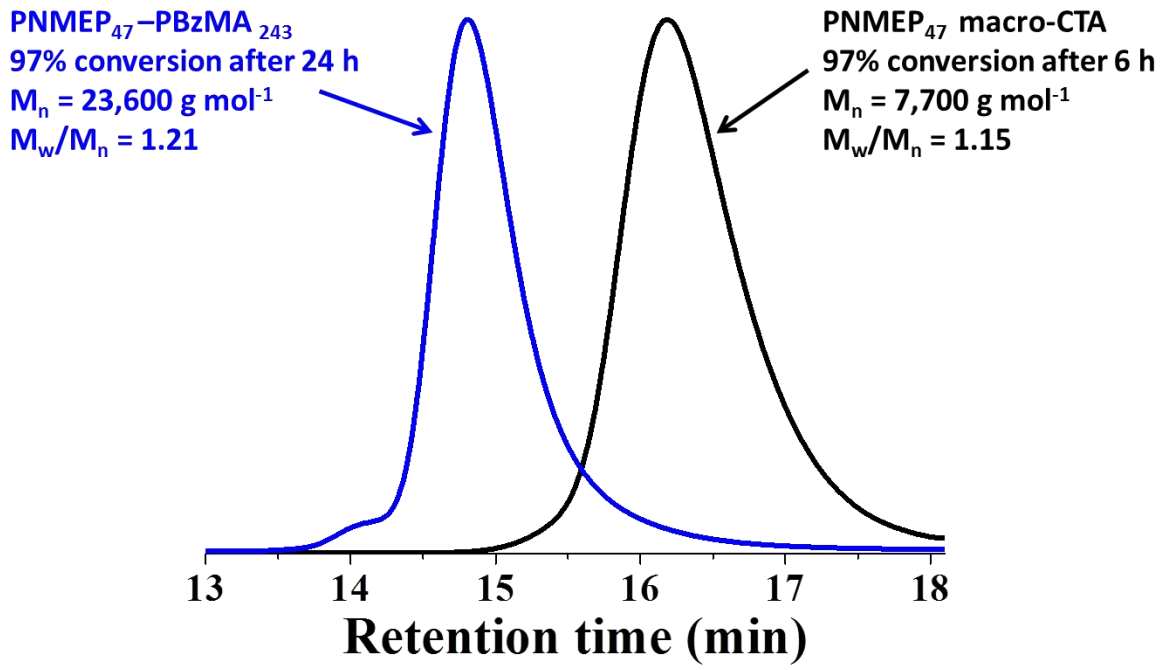

Figure 8. GPC analysis of the one-pot synthesis of $PNMEP_{47}$-$PBzMA_{243}$ at 70 °C. The black trace shows the $PNMEP_{47}$ macro-CTA after 6 h (97% conversion for an aliquot taken just before BzMA addition) synthesised using a CTA/initiator molar ratio of 3.0 at 60% w/w solids. The blue trace shows the $PNMEP_{47}$-$PBzMA_{243}$ diblock copolymer obtained after 24 h using a macro-CTA/initiator molar ratio of 5.0 at 30% w/w solids. (DMF eluent; refractive index detector; calibration using a series of near-monodisperse poly(methyl methacrylate) standards).